AIP | Journal of Applied Physics

Ge film growth in the presence of Sb by metal organic chemical vapor deposition

Ran-Young Kim, Ho-Gi Kim, and Soon-Gil Yoon

Citation: J. Appl. Phys. **102**, 083531 (2007); doi: 10.1063/1.2795673
View online: http://dx.doi.org/10.1063/1.2795673
View Table of Contents: http://jap.aip.org/resource/1/JAPIAU/v102/i8
Published by the American Institute of Physics.

Ge film growth in the presence of Sb by metal organic chemical vapor deposition

Ran-Young Kim and Ho-Gi Kim
Department of Materials Science and Engineering, Korea Advanced Institute of Science and Technology, 373-1 Guseong-dong, Daejeon 305-701, Korea

Soon-Gil Yoon[a)]
School of Nano Science and Technology, Chungnam National University, Daeduk Science Town, 305-764 Daejeon, Korea

(Received 4 July 2007; accepted 18 August 2007; published online 22 October 2007)

The germanium films were deposited on TiAlN bottom electrode at various temperatures by metal organic chemical vapor deposition using $Ge(allyl)_4(Ge(C_3H_5)_4)$ and $Sb(iPr)_3(Sb(C_3H_7)_3)$ precursors. Deposition of germanium films was only possible by a catalytic role of Sb metal by a thermal decomposition of $Sb(iPr)_3(Sb(C_3H_7)_3)$ precursors. Deposition rate of the Ge films increases with increasing Sb bubbling temperature at a substrate temperature of 370 °C. The deposition characteristics of Ge films were controlled by a surface reaction in the temperature range from 360 to 380 °C and were controlled by a mass transport in the range of 380–400 °C. The step coverage of Ge films in 500×200 nm^2 trench structure was approximately 93% at a substrate temperature of 370 °C. © *2007 American Institute of Physics*. [DOI: 10.1063/1.2795673]

I. INTRODUCTION

Recently, the demand for high speed, high density optical recording media using a direct overwrite scheme is very high. One of the most promising media for rewritable applications is phase change materials. Among several chalcogenide material candidates for the recording layer, $Ge_2Sb_2Te_5$ (GST) alloy film has been widely studied for this purpose as it has a direct overwrite capability within a short period of time.[1–3] It is reported that Ge–Sb–Te amorphous films crystallize into a single phase face-centered-cubic structure over a wide composition range even when film compositions do not match the exact stoichiometry of any of the reported compounds of $Ge_2Sb_2Te_5$, $GeSb_2Te_4$, or $GeSb_4Te_7$.[4,5] Strong interest has focused on the GST alloy materials for phase change random access memory (PRAM) because PRAM is most appropriate to the requirements such as nonvolatile, fast speed, high endurance among the next generation memories.

For PRAM applications, deposition of GST thin films by metal organic chemical vapor deposition (CVD) was already demonstrated by Kim *et al.*[6] In this study, precursors used for Ge, Sb, and Te in GST films are $Ge(allyl)_4[Ge(C_3H_5)_4]$, $Sb(iPr)_3[Sb(C_3H_7)_3]$, and $Te(iPr)_2[Te(C_3H_7)_2]$ colorless-liquid sources, respectively. However, quality of GST films reported in this study was very poor, resulting in difficulty to fill up the GST within the required trench structures. Accordingly, instead of a GST deposition by metal organic chemical vapor deposition (MOCVD) for gigabit PRAM applications, a study for the separate film deposition such as Ge, Sb, and Te is needed. First of all, this study examines Ge film growth for various deposition parameters. There are many precursors used for Ge film deposition such as $Ge(C_2H_5)_4$,[7] GeH_4,[8] etc. However, these precursors have drawbacks of a high decomposition temperature even though they have a high vapor pressure for CVD process. On the other hand, $Ge(allyl)_4$ precursors have advantages of low decomposition temperature (~243 °C) and an appropriate vapor pressure (1.45 mmHg at 50 °C), which is required for MOCVD process. Accordingly, in this study, film growth and morphologies of Ge films using $Ge(allyl)_4$ precursors are investigated as a function of growth temperature in the presence of Sb.

II. EXPERIMENT

Germanium thin films were prepared on TiAlN(30 nm)/SiO_2(100 nm)/Si substrates by MOCVD with bubbler types. Precursors used for Ge deposition are $Ge(allyl)_4$ $(Ge(C_3H_5)_4)$ and $Sb(iPr)_3(Sb(C_3H_7)_3)$ (DNF solution Co., Ltd., Korea) colorless-liquid sources. The bubbling temperature of $Ge(allyl)_4$ precursors was maintained at 50 °C and the $Sb(iPr)_3$ precursors was varied from 2 to 25 °C (vapor pressure of 0.06–0.4 mm Hg). The vapors of both Ge and Sb precursors were transported into the chamber by an argon carrier gas of 30 SCCM (SCCM denotes cubic centimeter per minute at STP), and H_2 of 150 SCCM was used as reactant gas to promote the decomposition of precursors. The mole fractions of Ge and Sb precursors are approximately 0.94 and 0.06, respectively. Deposition pressure was maintained at 25 Torr and relatively high operating pressures are checked by wide range diaphragm manometer (VRL, Vacuum Research Limited).

The crystallinity and structure of the Ge thin films were determined by x-ray diffraction (XRD) excited with Cu $K\alpha$ radiation. The microstructures and the composition of films were observed by scanning electron microscopy (SEM) and Auger electron spectroscopy (AES), respectively. The root mean square (rms) roughness of the films was measured by atomic force microscopy (AFM).

[a)]Author to whom correspondence should be addressed. Electronic mail: sgyoon@cnu.ac.kr

III. RESULTS AND DISCUSSION

Figures 1(a) and 1(b) show AFM images of Ge thin films deposited without and with an addition of $Sb(iPr)_3$ precursors, respectively, at a substrate temperature of 370 °C. When Ge thin films are deposited on TiAlN bottom electrode in the absence of antimony precursors, germanium films were not grown on TiAlN, as shown in Fig. 1(a). Germanium films were not grown on TiAlN as well as SiO_2 or Si substrates at various deposition temperatures (at 250–420 °C) and various vapor pressures of germanium precursor. As shown in Fig. 1(a), films deposited in the absence of Sb precursors show the same surface morphology as bare TiAlN bottom electrode, indicating rms roughness of approximately 1.0 nm. This means that Ge films are not grown on TiAlN in the absence of Sb precursors. On the other hand, as shown in Fig. 1(b), an addition of antimony precursors makes possible a film deposition, followed by rms roughness of approximately 2.5 nm. In order to ascertain the Ge film growth on TiAlN in the presence of Sb precursors, the elemental composition in the films was investigated by AES depth profile, as shown in Fig. 1(c). From the AES depth profile, germanium alone exists within the films and any antimony does not exist in the films. During the deposition of germanium, even if concentration of Sb source vapor was increased, Sb element did not exist in the films. The $Sb(iPr)_3$ precursors may be decomposed at earlier stage because the decomposition temperature (~160 °C) of Sb precursors is lower than that of Ge precursors used. This result suggests that Sb metal decomposed by Sb precursors plays an important role as catalyst for Ge deposition. In order to investigate indirectly the catalytic role of Sb metal for Ge film growth, the related experiment was performed. As a reference for Ge film growth, Fig. 2(A-a) shows x-ray diffraction pattern of Ge films grown on TiAlN/Si(001) substrates at 370 °C in the presence of Sb precursors by MOCVD. The Sb metal films with 50 nm thickness were deposited on TiAlN/Si substrates at 200 °C by rf sputtering, indicating at XRD patterns of Fig. 2(A-c). Figure 2(A-b) shows XRD pattern of the films grown using $Ge(allyl)_4$ precursors alone at 370 °C on Sb metal films in the absence of Sb precursors. As shown in Fig. 2(A-b), the films grown on Sb metal film exhibit the peak intensities showing Ge phase alone, even though the peak intensities are smaller than those shown in Fig. 2(A-a). In this case, peaks indicating Sb metal film are disappeared in XRD patterns. The XRD patterns of Fig. 2(A-b) suggest that the Ge deposition using $Ge(allyl)_4$ precursors is possible by a catalytic role of Sb metal decomposed from the Sb precursors. The elemental distribution for the films grown on Sb metal film was identified by AES depth profile shown in Fig. 2(b). The deposition of Ge on TiAlN/Si was clearly identified at AES depth profile and Sb element was not found in the layers. Even though the phase diagram for Ge–Sb alloy formation exists,[9] solubility limit of Sb into Ge lattice above 500 °C is very small, resulting in an impossibility of Ge–Sb alloy formation. The XRD results for the Ge–Sb alloy are not found in Ref. 10. In order to investigate the relationship between Sb metal film and hydrogen, the Sb metal film on TiAlN was maintained at 370 °C for 30 min in a hydrogen

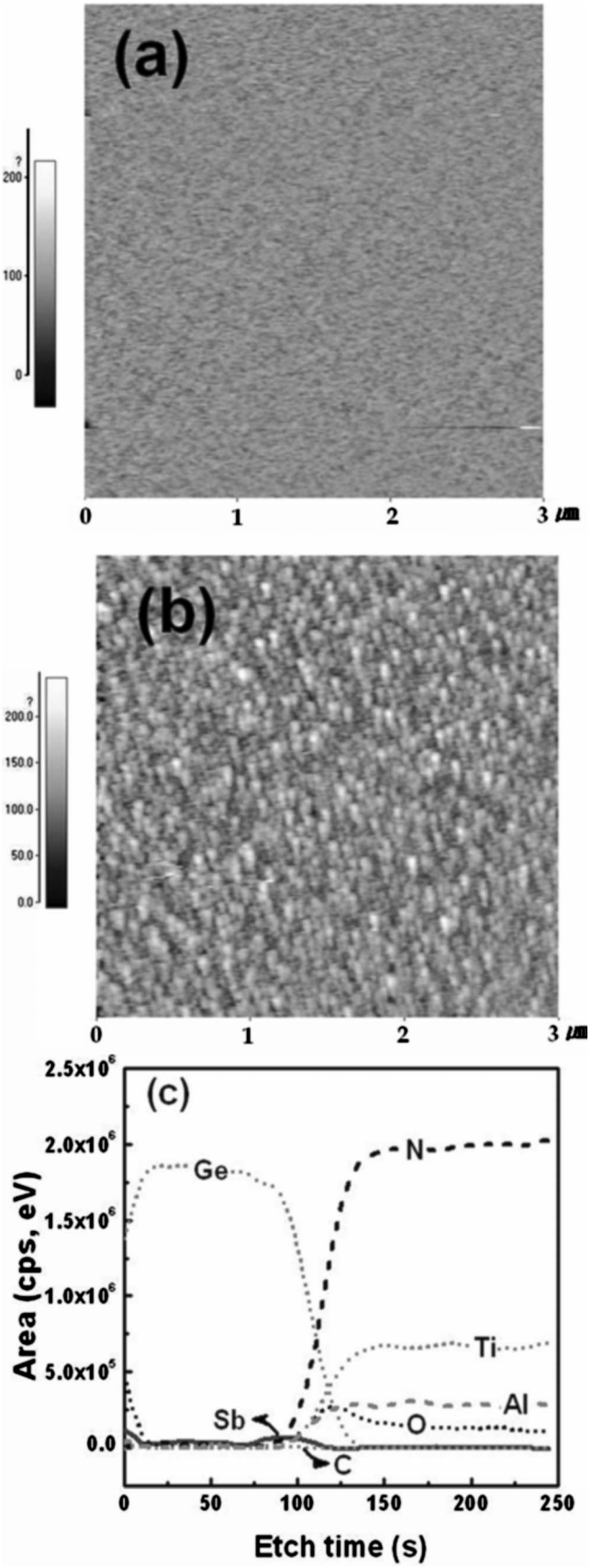

FIG. 1. AFM images of Ge thin films deposited at 370 °C for 2 h (a) without and (b) with an addition of $Sb(iPr)_3$ precursors, and (c) AES depth profile of the films deposited with $Sb(iPr)_3$ precursors.

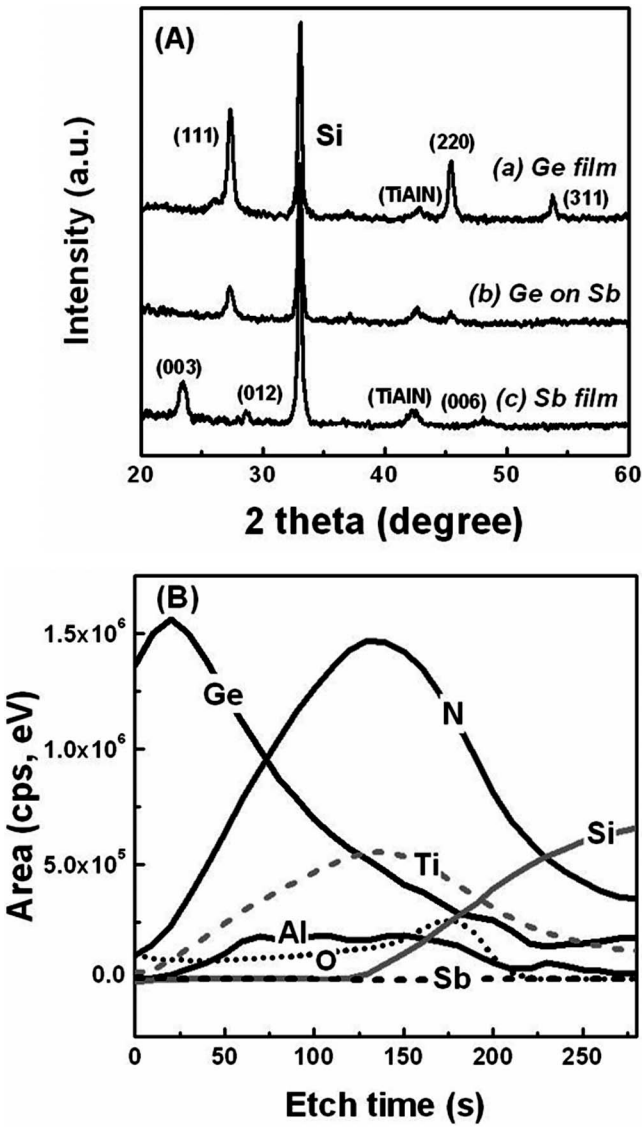

FIG. 2. (A-a) X-ray diffraction pattern of Ge films grown on TiAlN/Si(001) substrates at 370 °C in the presence of Sb precursors by MOCVD, (A-b) XRD pattern of Ge films grown using $Ge(allyl)_4$ precursors alone at 370 °C on Sb metal films in the absence of Sb precursors, and (A-c) XRD pattern of Sb metal films with 50 nm thickness deposited on TiAlN/Si substrates at 200 °C by rf sputtering. (B) AES depth profile showing the elemental distribution in Ge films grown in the absence of Sb precursors at 370 °C on Sb metal films deposited by rf sputtering.

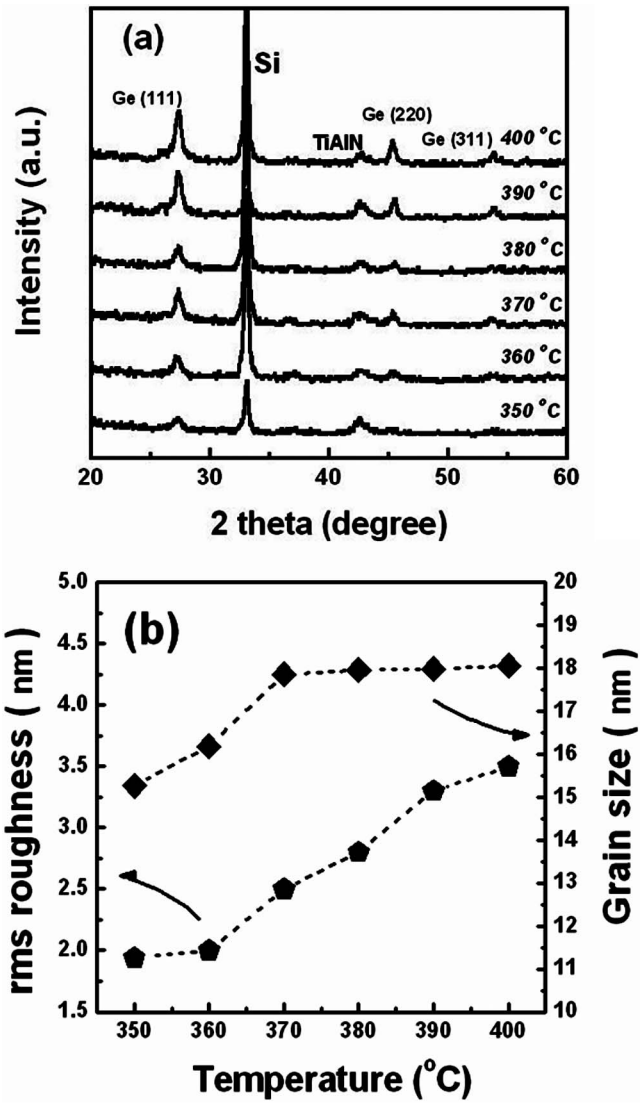

FIG. 3. (a) XRD patterns, (b) rms (root mean square) roughness and grain size of the Ge films deposited for 2 h at various temperatures [the bubbling temperature of Sb precursor is 5 °C (vapor pressure of 0.08 Torr)].

atmosphere. The Sb film on TiAlN was completely disappeared. This result suggests that the Sb film is evaporated by a reaction with hydrogen at 370 °C. This principle is consistently applied with the Ge film deposition in the presence of Sb precursors. In the result, this means that the Sb evaporated by a hydrogen play an important role as a catalyst for the deposition of Ge films on TiAlN. In this case, Sb does not include in the films. Accordingly, formation of $Ge_2Sb_2Te_5$ phase is possible by a reaction of Ge_2Te_2 and Sb_2Te_3 phases.

Figures 3(a) and 3(b) show XRD patterns and rms roughness, respectively, of Ge films deposited at various temperatures. As shown in Fig. 3(a), peak intensities of Ge films increase with increasing deposition temperature, and Sb metals were also not found in the films deposited at various temperatures. The deposited films show a polycrystalline nature at all of deposition temperature, and the films were not deposited below 350 °C in this experiment. As shown in Fig. 3(b), rms roughness of the films increases with increasing deposition temperature. An increase of rms roughness with increasing deposition temperature is related with an increase of grain size, as shown in Fig. 3(b). The grain size of the films was calculated with full width at half maximum of Ge (111) peaks using Scherrer's formula.[11]

Figures 4(a)–4(c) show x-ray diffraction patterns, rms roughness, and deposition rate, respectively, of Ge films deposited for 2 h at 370 °C with various bubbling temperatures of Sb precursor. The variations in bubbling temperature of Sb precursors from 2 to 25 °C mean the variations in vapor pressure of Sb precursors from 0.06 to 0.4 mmHg. The concentrations of Sb vapors were varied from 1.30×10^{-5} to 7.72×10^{-5} mol. The peak intensities of Ge films deposited at 370 °C become stronger with increasing Sb concentration by an increase of bubbling temperature, as shown in Fig. 4(a). This result makes clearly that antimony

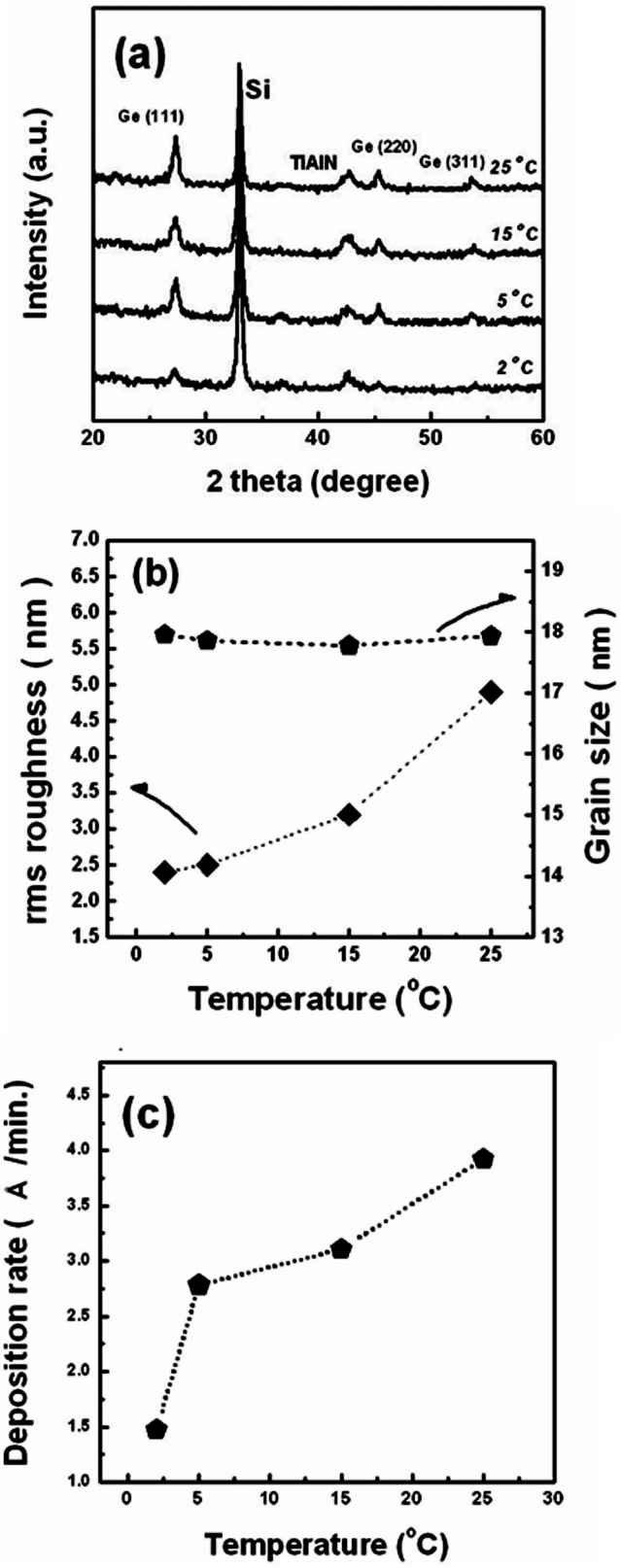

FIG. 4. (a) X-ray diffraction patterns, (b) rms roughness and grain size, and (c) deposition rate of Ge films deposited with various bubbling temperatures of Sb precursor (the deposition temperature of Ge films is 370 °C).

influences on the deposition characteristics of Ge films. As shown in Fig. 4(b), rms roughness of Ge films increases with increasing Sb bubbling temperature at a substrate temperature of 370 °C. On the other hand, grain size of the films was

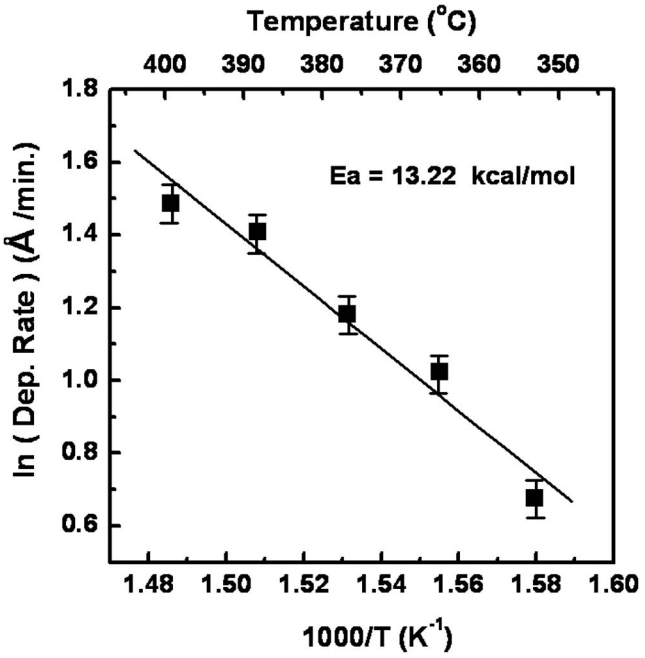

FIG. 5. Relationship between deposition rate and deposition temperature $(1/T)$ of the Ge films (the bubbling temperature of Sb precursor is 5 °C).

constantly maintained at 18 nm, irrespective of an increase of Sb bubbling temperature. This means that the grain size of the Ge films depends only on the variations in the deposition temperature. From this result, an increase of rms roughness of Ge films with increasing Sb bubbling temperature was due to an increase of the film thickness, as shown in Fig. 4(c). The deposition rate of the Ge films linearly increases with increasing Sb bubbling temperature.

The deposition characteristics of the Ge films were investigated with an Arrhenius plot between deposition rate and deposition temperature, as shown in Fig. 5. The Arrhenius equation is given as follows:

$$R = A \exp(-Q/kT), \tag{1}$$

where R, A, Q, k, and T are the deposition rate, a constant, the apparent activation energy, Boltzmann's constant, and Kelvin temperature, respectively. As shown in Fig. 5, the relationship between the deposition rate and the deposition temperature $(1/T)$ consists of a straight line in temperature range of 350–400 °C. In general, the deposition reaction is controlled by surface reaction when the apparent activation energy is between 10 and 50 kcal mol^{-1}, and by mass transport when the apparent activation energy is less than 10 kcal mol^{-1}.[12] As shown in the figure, the apparent activation energy obtained in the regions from 350 to 400 °C was approximately 13.22 kcal mol^{-1}. Hence the deposition reaction for Ge film growth was controlled by a surface reaction in the experimental regions.

Figures 6(a) and 6(b) show SEM images exhibiting step coverage of Ge films deposited on the trench structures of 500 nm in diameter and 200 nm in depth, 120 nm in diameter and 200 nm in depth, respectively. The step coverage is defined by a thickness ratio at height and bottom in the trench structure. The Ge films were deposited at the substrate temperature of 370 °C, Ge bubbling temperature of 50 °C,

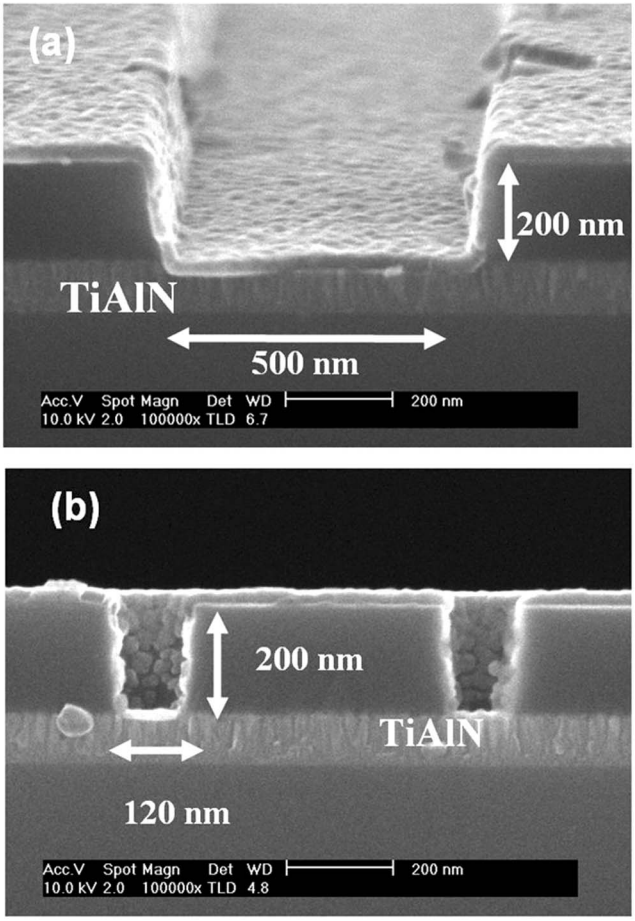

FIG. 6. SEM images of Ge films deposited on (a) 500×200 nm^2 and (b) 120×200 nm^2 trench structures. (The deposition temperature of Ge films is 370 °C and Sb bubbling temperature of 5 °C.)

and Sb bubbling temperature of 5 °C. The thickness of Ge films was approximately 40 nm. As shown in in Fig. 6(a), the step coverage in trench structure of 500 nm in diameter and 200 nm in depth was approximately 93%. On the other hand, the step coverage in trench structure of 120 nm in diameter and 200 nm in depth was a little poor, indicating about 80%.

IV. CONCLUSIONS

Deposition of the germanium films by MOCVD using $Ge(allyl)_4(Ge(C_3H_5)_4)$ precursors is possible by a catalytic role of Sb metal decomposed from the $Sb(iPr)_3$ precursors. Deposition rate of the Ge films increases with increasing Sb bubbling temperature at a substrate temperature of 370 °C. The deposition of Ge films was controlled by a surface reaction in the temperature range from 360 to 380 °C and by a mass transport in the range of 380 to 400 °C. The step coverage of Ge films in 500×200 nm^2 trench structure was approximately 93% at a substrate temperature of 370 °C.

ACKNOWLEDGMENTS

This research was partly supported by the Brain Korea 21 project in 2006 and by the Korea Science and Engineering Foundation through the Research Center for Advanced Magnetic Materials at Chungnam National University.

[1] J. Gonzalez-Hernandez, B. S. Chao, D. Strand, S. R. Ovshinsky, D. Pawlik, and P. Gasiorowski, Appl. Phys. Commun. **11**, 557 (1992).
[2] N. Yamada, E. Ohno, K. Nishiuchi, N. Akahira, and M. Takao, J. Appl. Phys. **69**, 2849 (1991).
[3] T. H. Jeong, M. R. Kim, H. Seo, S. J. Kim, and S. Y. Kim, J. Appl. Phys. **86**, 774 (1999).
[4] K. A. Agaev and A. G. Talybov, Sov. Phys. Crystallogr. **11**, 400 (1966).
[5] I. I. Petrov, R. M. Imamovet, and Z. G. Pinsker, Sov. Phys. Crystallogr. **13**, 339 (1968).
[6] R. Y. Kim, H. G. Kim, and S. G. Yoon, Appl. Phys. Lett. **89**, 102107 (2006).
[7] J. E. Boucham, M. Amjould, R. Morancho, F. Maury, and A. Yacoubi, Ann. Chim. Sci. Mat. **23**, 381 (1998).
[8] D. Buttard, G. Dolino, Y. Campidelli, and A. Halimaoui, J. Cryst. Growth **183**, 294 (1998).
[9] E. A. Brandes, *Smithells Metals Reference Book*, 6th ed. (Robert Hartnoll, Bodmin, 1983), Chap. 11, p. 283.
[10] International Center for Diffraction Data, Newtown Square, PA, Powder Diffraction File, formerly JCPDS.
[11] B. D. Cullity, *Elements of X-ray diffraction*, 2nd ed. (Addison-Wesley, Reading, MA, 1978), Chap. 3, p. 102.
[12] D. W. Shaw, *Crystal Growth* (Plenum, London, 1974), p. 11.